Nano World Journal

https://doi.org/10.17756/nwj.2023-s1-083

Research Article

Open Access

Performance Analysis of Solar Biomass-based Hybrid Microgrid System Coupled with EFGT and Organic Rankine Cycle in India

Ayona Biswas* **and Aritra Ganguly**

Indian Institute of Engineering Science and Technology, Shibpur, West Bengal, India

***Correspondence to:**
Ayona Biswas
Indian Institute of Engineering Science and Technology, Shibpur, West Bengal, India.
E-mail: ayonabiswas123@gmail.com

Received: November 24, 2022
Accepted: April 23, 2023
Published: April 25, 2023

Citation: Biswas A, Ganguly A. 2023. Performance Analysis of Solar Biomass-based Hybrid Microgrid System Coupled with EFGT and Organic Rankine Cycle in India. *NanoWorld J* 9(S1): S433-S439.

Published by United Scientific Group

Abstract

Various non-conventional energy sources, *viz.* solar, wind, hydro, and biomass, have become the most encouraging environmentally friendly power sources fulfilling world energy needs. But, due to climate change and the uncertainty of wind and solar energy sources, hybrid microgrid systems have become very common in India. In the present paper, a solar biomass-based hybrid microgrid system coupled with EFGT (Externally Fired Gas Turbine) and ORC (Organic Rankine Cycle) is framed to attain the total electricity demand of a village in the Indian context. We carry out energy-exergy-based analyses to investigate the system's performance. A fixed bed downdraft type gasifier is used with EFGT to increase the system's thermal performance. A PTC (Parabolic Trough Collector) and Therminol-VP1 are used in the solar circuit as the solar collector and heat transfer fluid, respectively. Furthermore, six working fluids, *viz.* o-xylene, toluene, ethylbenzene, n-octane, and n-nonane are scrutinized based on their thermochemical properties, and availability in the Indian market to conduct the parametric analyses. The operating temperatures of the system are 265 and 290 for solar and biomass-assisted circuits, respectively. The parametric studies reveal that o-xylene gave the best performance, while n-heptane gave the worst performance. We also observe that EFGT-based downdraft gasifier and PTC are the prime sources of exergy destruction.

Keywords

Organic Rankine cycle, Gasifier, Externally fired gas turbine, Working fluids, Parabolic trough solar collector, Exergy

Introduction

The concept of a microgrid in the power generation sector has become most popular globally due to its contribution to clean and sustainable development. For the last few decades, India has experienced significant growth in electricity generation and demand due to rapid urbanization and population growth. Currently, India's coal-based thermal power plant contributes a substantial portion of total power generation to fulfill the growing electricity demand. The contribution of coal-based conventional power plants is 54% of total electricity demand, whereas renewable energy sources such as solar, wind, and hydropower systems contribute only 34% [1]. Due to a plethora of challenges associated with the existing conventional coal-based energy production systems like emissions of CO_2, exhaust gases, environmental hazards, transportation problems, and lack of power storage, Government bodies and scientific organizations have come up with an alternative approach to electrification in rural and semi-urban regions. In India, energy demand is accelerated with the rapid growth of the economy. It is expected that the installed capacity in India will be further augmented to 800 GW by 2032 [2].

Several studies have been reported using various simulation software like Engineering Equation solver, Hybrid Optimization Model for Multiple Energy Resources, and MATLAB to reveal the benefits of hybrid microgrid systems. Al-Ghussain et al. [3] worked on an integrated photovoltaic-wind-biomass-based hybrid microgrid system to produce 100% renewable energy for fulfilling the electricity demands of a university campus in the USA. Neto et al. [4] investigated the complementarity of solar, wind, and tidal system in an isolated hybrid microgrid in a case study in the coastal zone of northern Brazil. Kaur et al. [5] worked on a techno-economic analysis of a photovoltaic (PV)-biomass-based microgrid system. Their study proposed a microgrid system for effectively utilizing available renewable resources like crop residue, mainly organic compounds, for reliable rural electrification. Das et al. [6] worked on metaheuristic optimization techniques for the techno-economic optimization of an off-grid hybrid renewable energy system used for a radio transmitter unit in the Indian context. They used metaheuristic techniques as this technique helps to achieve quick, accurate, and optimal solutions. Bukar et al. [7] worked on a PV-wind-battery-diesel-generator-based microgrid system to obtain optimum sizing parameters using the Grasshopper swarm optimization technique. They compared the result of this optimization technique with the Particle swarm optimization and Cuckoo search optimization technique. Javed et al. [8] carried out a techno-economic analysis of a standalone solar-wind-battery hybrid system integrated with energy storage to optimize the system for an off-grid area with the help of a genetic algorithm. Ayop et al. [9] worked on component sizing of a standalone photovoltaic system. Ogujuyigbe et al. [10] worked on a PV-wind-split-diesel-battery-based hybrid microgrid system to minimize the total cost of the life cycle, reduce carbon emission and dump energy for residential complexes of remote areas and optimize the sizing parameters. Kumaravel et al. [11] carried out a techno-economic study on biomass-based hybrid microgrid systems to address their feasibility in rural areas. Borhanazad et al. [12] optimized a microgrid system using Multi-Objective Particles Swarm Optimization.

Several numerical works have been performed on the cost modelling and energy optimization of the microgrid system using various simulation software (*viz*. Engineering Equation solver and MATLAB) and optimization techniques. In this article, performance analysis of solar biomass microgrid system has been carried out from the thermodynamic point of view. In great detail, this paper examines the energy and exergy of a solar biomass-based organic Rankine cycle with a high critical temperature working fluid. Six different organic working fluids (o-xylene, toluene, ethylbenzene, n-octane, n-heptane, and n-nonane) are shortlisted to find the net electrical efficiency, work output, and exergy efficiency of an S-ORC system. Finally, the study reveals that the turbine inlet and outlet temperatures are the major performance parameters from energy-exergy-based analyses. EFGT is introduced in the present scheme to increase the system's thermal performance.

System Modeling

A solar biomass-based hybrid microgrid system coupled with an externally fired gas turbine (EFGT) and ORC is shown in figure 1 to fulfill the electricity demand and CHP applications. The system consists of five sub-systems. Those are: 1) Downdraft gasifier sub-system 2.) EFGT (Externally Fired Gas Turbine) sub-system 3) Solar collector-based sub-system, 4) Organic Rankine cycle (ORC) subsystem, and 5) CHP subsystem.

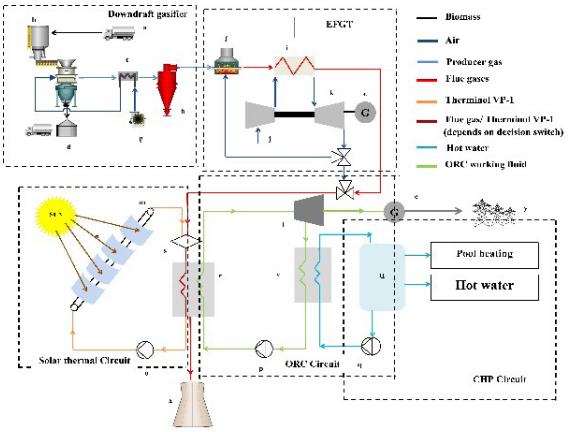

Figure 1: Schematic diagram of solar-biomass-based hybrid microgrid system coupled with EFGT and organic Rankine cycle. **a.** Biomass storage, **b.** Reactor, **c.** air pre-heater, **d.** Biomass valorization system, **e.** Generator, **f.** External combustion chamber, **g.** Air blower, **h.** Cyclone, **i.** High temperature heat exchanger, **j.** Compressor, **k.** Turbine-1, **l.** Turbine-2, **m.** Receiver, **n.** Parabolic trough collector, **o.** Circulation pump-1, **p.** Polypropylene pump, **q.** Circulation pump-2, **r.** Evaporator, **s.** Decision switch, **u.** Hot water tank, **v.** Condenser, **x.** Cooling tower, and **y.** Microgrid.

Down-draft gasifier modeling

This subsystem consists of a down-draft gasifier, biomass storage, air pre-heater, biomass valorization system, and cyclone. In this current study, a fixed bed down-draft type gasifier is used. Food waste with 5 - 60% moisture content is used as biomass [13]. After entering the reactor, the moisture content of the biomass releases as water vapor due to drying-pyrolysis, which increases the process temperature. After drying-pyrolysis, char (solid substance), some volatile substances such as H_2, CO_2, CO, CH_4, and tar (liquid substance) are produced from biomass. After reaching the combustion-reduction zone, controlled combustion occurs with the presence of pre-heated air, and the temperature increases up to 600 °C. Tar gets converted into H_2, H_2O, CO_2, CO, and CH_4 at high temperatures. Finally, the producer gas leaves the gasifier, which is passed through the cyclone to remove dust particles and particulates. Biochar characteristics of the selected biomass are shown in table 1.

EFGT subsystem modeling

This sub-system consists of an external combustion chamber where the producer gas is burnt at atmospheric pressure, a high-temperature heat exchanger where the thermal energy is transferred to the clean air from flue gases, and compressor-turbine pair which is interconnected with a shaft and connects with an electric generator. The producer gas is not compressed here to avoid high electrical consumption. A portion of the hot air is recirculated from the turbine's outlet towards the combustion chamber through a control valve to increase the system's thermal performance. Flue gases from

Table 1: Biochar characteristics of biomass [13].

Source of the biomass	Food waste with 5 - 60% moisture
Fixed carbon	10.18 - 13.09
C (%)	20.28 - 21.43
H (%)	0.05 - 0.78
O (%)	0.53 - 2.31
N (%)	2.34 - 3.12
H/C	2.17 - 34.30
O/C	11.68 - 51.75
Ash content (%)	72.27 - 74.09
Char yield (%)	33.57 - 30.19

the high-temperature heat exchanger and hot air from the outlet of the turbine are mixed and reach approximately 290 °C. This waste heat will increase the ORC subsystem's thermal efficiency.

Solar circuit modelling

Solar collector based sub-system consists of a solar collector, a circulation pump, and heat transfer fluid. Parabolic trough collector is used as solar collector and Therminol VP-1 is selected as the heat-transfer fluid for the solar circuit. This oil is selected for its excellent heat transfer properties and utilized for its properties and for the temperature control and therefore used in 4 various power generation plants as a heat transfer fluid for parabolic troughs for power generation.

ORC subsystem modeling

The turbine, condenser, evaporator, and pump are the four major components of the Rankine cycle. The ORC is connected to the solar field of the parabolic trough collector or the EFGT subsystem through the evaporator. Due to the uncertainty in the availability of sunlight, a decision switch is placed before the evaporator. If the total solar irradiance is less than 400 W/m^2, then the ORC circuit will be connected with the EFGT subsystem. Parameters used in the simulation are shown in table 2.

CHP subsystem modeling

This subsystem is used for space heating and pool heating. A circulation pump circulates the water to the condenser, and hot water is stored in a tank.

Mathematical Modeling

Energy modeling

Solar collector modeling

The heat received by the solar collector is transferred to the heat transfer fluid. Energy balance equation of the solar circuit is shown as:

$$Q_E = G_b A_{Col} \eta_{Col} = m_{htf} C_{p,htf} \left(T_{Col,out} - T_{Col,in}\right) \quad (1)$$

The thermal efficiency of parabolic trough solar collector can be expressed as:

Table 2: Parameters used in the simulation.

Parameters	Values with units
Organic Rankine Cycle	
Pump's efficiency (isentropic)	85%
Expander's efficiency (isentropic)	75%
Pump's inlet temperature	100 °C
Expander's inlet pressure	2 MPa
Parabolic Trough Collector	
Mass flow rate of the thermal oil	2 kg/s
Collector's width	12.27 m
Collector's length	5.57 m
Cover's inner diameter	0.12 m
Cover's outer diameter	0.125 m
Receiver's inner diameter	0.066 m
Receiver's outer diameter	0.07 m
Total solar irradiance	0.55 kW/m^2
Optical efficiency	0.8
Number of rows	100
Number of collectors	10
Ambient temperature	25 °C

$$\eta_{Col} = a_0 - a_1 \frac{\left(T_{Col,m} - T_{amb}\right)}{G_b} - a_2 \frac{\left(T_{Col,m} - T_{amb}\right)^2}{G_b} \quad (2)$$

In the above equation, a_0, a_1, and a_2 are the constant of the PTC.

Gasifier and EFGT sub-system modeling

In equation 3, the global gasification equation is shown as:

$$CH_aO_bN_cS_dAsh + w(H_2O) + e(O_2 + 3.76N_2) \rightarrow x_1H_2 + x_1CO + x_3H_2O + x_4CO_2 + x_5CH_4 + x_6N_2 + x_7C + x_8Ash \quad (3)$$

To enhance thermal energy utilization, producer gas can be burnt at the outlet of the EFGT. For this case, sensible heat at the outlet of the gasifier can be considered; gasification efficiency can be calculated using the following expression:

$$\varsigma_{gasi} = \varsigma_{hot} = \frac{m_{pg}\left(LHV_{pg} + C_p \Delta T\right)}{m_b LHV_b} \quad (4)$$

The gasification efficiency can be calculated as:

$$\varsigma_{gasi} = \varsigma_{cold} = \frac{m_{pg} LHV_{pg}}{m_b LHV_b} \quad (5)$$

The electrical efficiency of the EFGT subsystem can be expressed as:

$$\eta_{e,EFGT} = \frac{(P_t - P_c)\eta_g}{m_b LHV_b} \quad (6)$$

ORC modeling

The thermal analysis of the overall system and subsystem is based on some basic assumptions, which are as follows [14]:

- Steady-state operating condition.
- No heat loss and pressure drop throughout the system.
- Negligible change in K.E and P.E.
- Saturated condition at evaporator and condenser's outlet.
- The pump and expander are adiabatic with constant isentropic efficiency.

$$Q_e - Q_c + W_p - W_t = 0 \quad (7)$$

The two laws behind the functioning of the Rankine cycle are the conservation of mass and the energy that is used to simulate the subsystem of ORC. The amount of heat added to the evaporator can be expressed as:

$$Q_e = m_f (h_2 - h_1) \quad (8)$$

Heat rejected by the condenser can be written as:

$$Q_c = m_f (h_3 - h_4) \quad (9)$$

The mechanical power generated by the turbine can be expressed as:

$$W_t = m_f (h_2 - h_3) \quad (10)$$

The ORC pump's power consumption can be calculated as follows:

$$W_P = m_f (h_1 - h_4) \quad (11)$$

The solar-powered ORC's net electric power can be given by:

$$W_{net,el} = W_t - \frac{W_p}{\eta_{motor}} \quad (12)$$

The system's net electric efficiency can be expressed as:

$$\eta_{el} = W_{net,el} / Q_e \quad (13)$$

Exergy modeling

At steady state conditions, the exergy balance of a control volume can be defined as [14]:

$$\sum \left(1 - \frac{T_0}{T_k}\right) Q_k - W - \sum_{in} \dot{m}\phi - \sum_{out} \dot{m}\phi = 0 \quad (14)$$

The flow of exergy per unit mass flow rate can be written as [14]:

$$\phi = (h - h_0) - T_0 (S - S_0) + \left(\frac{\tilde{a}^2 - V_0^2}{2}\right) + g(z - z_0) \quad (15)$$

The net electrical exergy efficiency of the organic Rankine cycle can be expressed as:

$$\eta_{exergy,el} = \frac{W_{net}}{E_{\dot{x},in}} \quad (16)$$

Inflow exergy of the system can be defined by the equation (17) [17]:

$$E_{\dot{x},in} = A_{ap,total} G_b \left(1 + \frac{1}{3}\left(\frac{T_0}{T_s}\right)^4 - \frac{4}{3}\left(\frac{T_0}{T_s}\right)\right) \quad (17)$$

Each component of a solar-powered ORC system has an irreversibility ratio of [18]:

$$IR = \frac{E_{\dot{x},d}}{E_{\dot{x},d,total}} \quad (18)$$

Another important factor in studying turbine size characteristics in an organic Rankine cycle system is the turbine size parameter (SP) [19]:

$$SP = \sqrt{V_3} / \sqrt[4]{\Delta h} \quad (19)$$

The chemical energy of the biomass can be expressed as:

$$E_{\dot{x},b,ch} = \beta LHV_b \quad (20)$$

Exergy input for the biomass-based system can be expressed as:

$$E_{\dot{x},b} = m_b LHV_b \quad (21)$$

Results and Discussion

Model validation

The findings of the developed model for the solar collector are reported in this section, and the same is compared with a reference study Muoz-Anton et al. [15] available in the literature to validate the current solar model. It is observed that a marginal deviation of 1 - 2 percent was observed.

The next step is to compare the model's performance with the study where fluids have been used as the heat transfer fluid. The research done by Blanco et al. [20] was picked as the most reasonable for looking at the current model. Bellos [16] has also confirmed his findings from Blanco et al. [20]. The proposed model has been validated using both literature sources, indicating that it is accurate and suitable for further research. The results of a comparison for a vast operation range are shown in figure 2. It is observed that the results predicted by our model and that of the reference are close to each other.

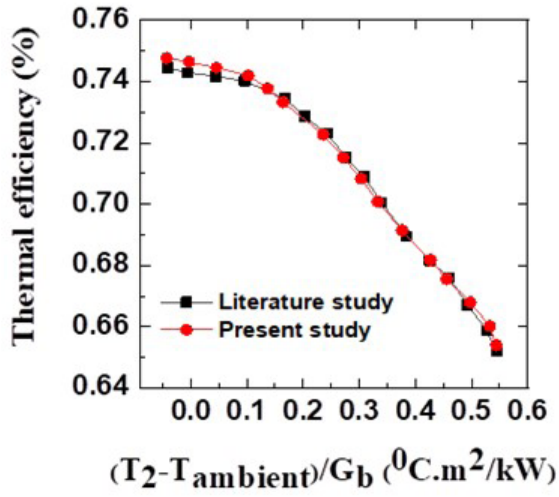

Figure 2: Validation of current model with literature study [20] for thermal oils.

As a result, the correctness of the version is accepted. As a result, the correctness of the model is accepted.

Resource and load assessment

A case study is done on a Punjab village at 30.5° latitudes and 76.5° longitude. Data have been collected from NASA's surface metrology and solar energy database [5]. The locality has an average solar irradiance of 544 Wh/m²/day with an average clearance index of 63.3%. The locality has approximately 300 sunny days in a year [5]. The primary biomass sources are rice, wheat, maize, and food waste. According to data collected from various surveys, the village has ample numbers of animals. 0.6 - 0.8 m^3 biogas can be produced from 1 kg of cow dung, producing 1.5 kWh electric energy. In the village, the average scale of biomass is around 8 tons/month, except for the months of harvesting the rice and wheat. The availability of biomass is shown in figure 3 [5]. The village power requirement for a day is shown in figure 4 during the summer and winter seasons.

Shortlisting of working fluid

O-xylene, ethylbenzene, toluene, N-nonane, N-octane, and N-heptane are shortlisted based on their physical and chemical properties, environmental impact, and availability in the Indian market.

Simulation method

After scrutinizing six organic working fluids, several numerical simulations are carried out using DWSIM, open-source process simulation software. The thermodynamic properties data of the working fluids are collected from NIST Reference Fluid Thermodynamic and Transport Properties Database version 8. During the parametric studies, the expansion ratios of the organic fluids vary from 20 - 140 and volumetric flow rates vary from 0.6 - 3 m^3/s. The inlet temperatures of the turbine are within the range of 255 - 300 °C. The pressure drop across the evaporator is neglected during the simulations.

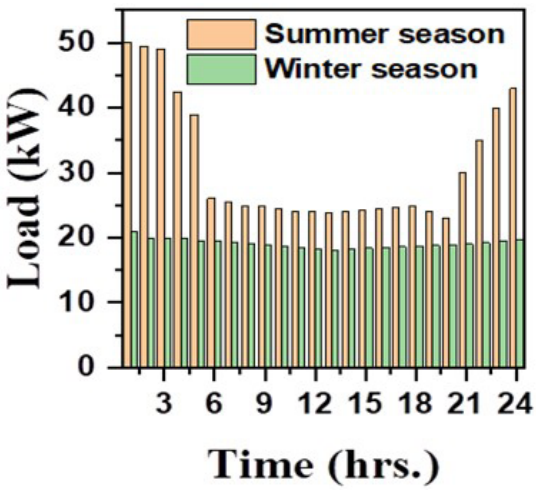

Figure 3: Load demands per day.

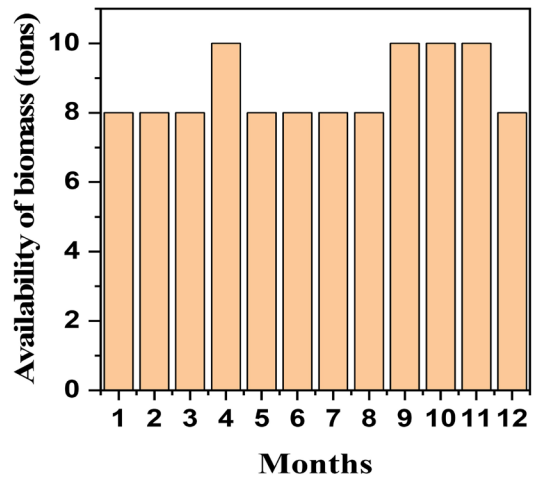

Figure 4: Availability of biomass throughout the year.

Impact of inlet temperature fluctuations on net electrical power and efficiency

The variation of net electrical power production and efficiency with turbine inlet temperature for the different fluids considered is shown in figure 5 and figure 6. It is observed that the organic fluid o-xylene, gives the best electrical efficiency due to its lower condenser pressure. On the other hand, n-heptane has the least electric efficiency and power production due to higher condenser pressure.

Impact of inlet temperature fluctuations on system exergetic performance

The variation of exergy efficiency and total exergy destruction rate with the turbine inlet temperature for the different fluids are shown in figure 7 and figure 8. It can be observed from figure 7 that exergy efficiency and electrical efficiency increase when the inlet temperature of the turbine increases. Similar behaviour is observed for the exergy loss for the three fluids; that is, with the change in the inlet temperature of the turbine, exergy efficiency for the fluids increases. In addition, as shown in figure 8, the total exergy destruction rate decreases when the inlet temperature of the turbine

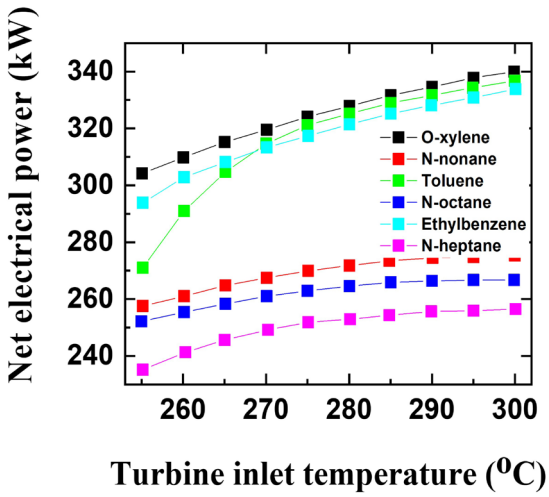

Figure 5: Variation of net electrical power with turbine inlet temperature at 120 °C condenser inlet temperature.

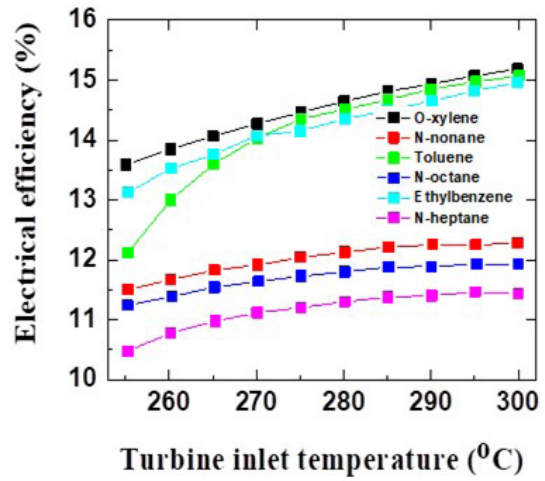

Figure 6: Variation of net electrical efficiency with turbine inlet temperature at 120 °C condenser inlet temperature.

is increased. In a fashion similar to electrical efficiency and power production, we see that the fluid o-xylene has elevated exergy efficiency, whereas, on the other hand, n-heptane is the fluid with the least efficiency.

Impact of turbine inlet temperature fluctuations on the rate of the exergy destruction

The variation in rate of exergy destruction with the turbine inlet temperature is shown in figure 9. From figure 9 it is observed that the pace of exergy destruction of the ORC component and overall exergy regarding the inlet temperature of the turbine. It is understood from the figure that the biomass gasifier and solar collectors annihilate most of the exergy, and as the inlet temperature of the turbine ascents, the exergy loss comes down. Exergy destruction is less in the other parts of the system.

Conclusions

In the current study, a comprehensive exergy and energy analysis of a solar biomass-based microgrid was performed using the organic Rankine cycle and EFGT. For evaluation,

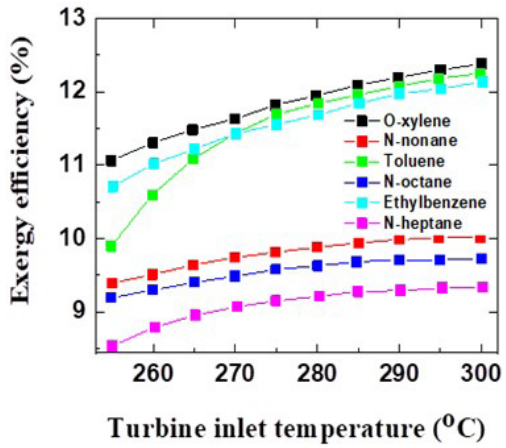

Figure 7: Variation of exergy efficiency with turbine inlet temperature at 120 °C condenser inlet temperature.

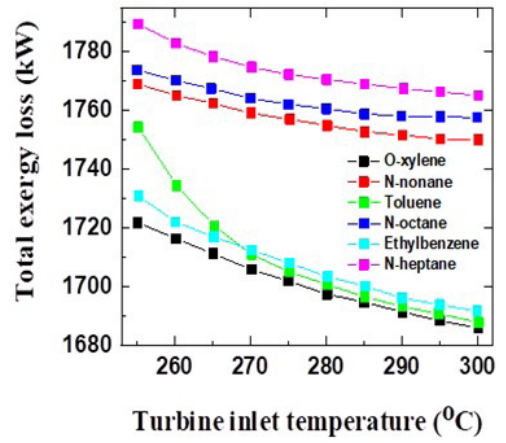

Figure 8: Variation of total exergy destruction rate with turbine inlet temperature at 120 °C condenser inlet temperature.

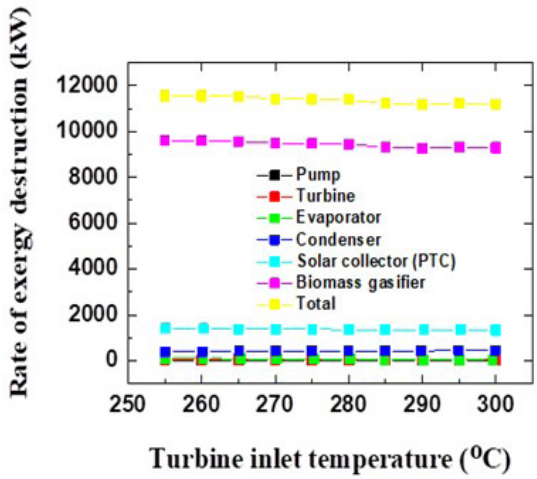

Figure 9: Variation of total exergy destruction rate with turbine inlet temperature at 120 °C condenser inlet temperature.

six hydraulic fluids: o-xylene, toluene, ethylbenzene, n-octane, heptane, and n-nonane, were considered. The study reveals the following:

- Increasing turbine inlet temperature improves net elec-

trical power and exergy efficiency and reduces the overall destruction rate.

- The fluid o-xylene has the highest exergy and energy performance of the six liquids, while heptane has the lowest exergy and energy performance. O-xylene gives 15.2% and 12.4% energy and exergy efficiency, respectively, at 300 turbine's inlet temperature and 120 condenser's inlet temperature. N-heptane gives 11.4% and 9.34% energy and exergy efficiency, respectively, under the same operating condition.
- Parabolic trough collector and EFGT-based downdraft gasifier are the reason for the destruction of the exergy. The exergy destruction and irreversibility ratio of parabolic through collectors are 1398.2 KW and 12.1%, respectively, at 255 turbine's inlet temperature. For EFGT-based downdraft gasifier, exergy destruction and irreversibility ratio are 11551.26 KW and 83%, respectively.
- The study reinforces the need and viability of microgrid systems for the developing countries like India.

Acknowledgements

None.

Conflict of Interest

The authors declare no conflict of interests that are relevant to the content of this article.

Credit Author Statement

Ayona Biswas: Writing - original draft preparation; Aritra Ganguly: Supervision. All the authors read and approved the manuscript.

References

1. Central Electricity Authority. All India Installed Capacity (in MW) of Power Stations. [https://cea.nic.in/wp-content/uploads/2020/02/installed_capacity-12-2.pdf] [Accessed April 24, 2023]
2. Singh J. 2016. A roadmap for production of sustainable, consistent and reliable electric power from agricultural biomass-an Indian perspective. *Energy Policy* 92: 246-254. https://doi.org/10.1016/j.enpol.2016.02.013
3. Al-Ghussain L, Ahmad AD, Abubaker AM, Mohamed MA. 2021. An integrated photovoltaic/wind/biomass and hybrid energy storage systems towards 100% renewable energy microgrids in university campuses. *Sustain Energy Technol Assess* 46: 101273. https://doi.org/10.1016/j.seta.2021.101273
4. Neto PBL, Saavedra OR, Oliveira DQ. 2020. The effect of complementarity between solar, wind and tidal energy in isolated hybrid microgrids. *Renew Energy* 147: 339-355. https://doi.org/10.1016/j.renene.2019.08.134
5. Kaur M, Dhundhara S, Verma YP, Chauhan S. 2020. Techno-economic analysis of photovoltaic-biomass-based microgrid system for reliable rural electrification. *Int Trans Electr Energy Syst* 30(5): e12347. https://doi.org/10.1002/2050-7038.12347
6. Das M, Singh MAK, Biswas A. 2019. Techno-economic optimization of an off-grid hybrid renewable energy system using metaheuristic optimization approaches–case of a radio transmitter station in India. *Energy Convers Manag* 185: 339-352. https://doi.org/10.1016/j.enconman.2019.01.107
7. Bukar AL, Tan CW, Lau KY. 2019. Optimal sizing of an autonomous photovoltaic/wind/battery/diesel generator microgrid using grasshopper optimization algorithm. *Sol Energy* 188: 685-696. https://doi.org/10.1016/j.solener.2019.06.050
8. Javed MS, Song A, Ma T. 2019. Techno-economic assessment of a stand-alone hybrid solar-wind-battery system for a remote island using genetic algorithm. *Energy* 176: 704-717. https://doi.org/10.1016/j.energy.2019.03.131
9. Ayop R, Isa NM, Tan CW. 2018. Components sizing of photovoltaic stand-alone system based on loss of power supply probability. *Renew Sustain Energy Rev* 81: 2731-2743. https://doi.org/10.1016/j.rser.2017.06.079
10. Ogunjuyigbe ASO, Ayodele TR, Akinola OA. 2016. Optimal allocation and sizing of PV/Wind/Split-diesel/Battery hybrid energy system for minimizing life cycle cost, carbon emission and dump energy of remote residential building. *Appl Energy* 171: 153-171. https://doi.org/10.1016/j.apenergy.2016.03.051
11. Kumaravel S, Ashok S, Balamurugan P. 2012. Techno-economic feasibility study of biomass based hybrid renewable energy system for microgrid application. In International Conference on Green Technologies, Trivandrum, India.
12. Borhanazad H, Mekhilef S, Ganapathy VG, Modiri-Delshad M, Mirtaheri A. 2014. Optimization of micro-grid system using MOPSO. *Renew Energy* 71: 295-306. https://doi.org/10.1016/j.renene.2014.05.006
13. Wang N, Chen Q, Zhang C, Dong Z, Xu Q. 2022. Improvement in the physicochemical characteristics of biochar derived from solid digestate of food waste with different moisture contents. *Sci Total Environ* 819: 153100. https://doi.org/10.1016/j.scitotenv.2022.153100
14. Cengel YA, Boles MA, Kanoğlu M. 2011. Thermodynamics: An Engineering Approach. McGraw-hill, New York.
15. Muñoz-Anton J, Biencinto M, Zarza E, Díez LE. 2014. Theoretical basis and experimental facility for parabolic trough collectors at high temperature using gas as heat transfer fluid. *Appl Energy* 135: 373-381. https://doi.org/10.1016/j.apenergy.2014.08.099
16. Bellos E, Tzivanidis C, Antonopoulos KA. 2017. A detailed working fluid investigation for solar parabolic trough collectors. *Appl Therm Eng* 114: 374-386. https://doi.org/10.1016/j.applthermaleng.2016.11.201
17. Petela R. 2005. Exergy analysis of the solar cylindrical-parabolic cooker. *Sol Energy* 79(3): 221-233. https://doi.org/10.1016/j.solener.2004.12.001
18. Bejan A, Tsatsaronis G, Moran MJ. 1995. Thermal Design and Optimization. John Wiley & Sons.
19. Macchi E, Perdichizzi A. 1981. Efficiency prediction for axial-flow turbines operating with nonconventional fluids. *J Eng Power* 103(4): 718-724. https://doi.org/10.1115/1.3230794
20. Blanco J, Alarcón D, Sánchez B, Malato S, Maldonado MI, et al. 2003. Technical comparison of different solar-assisted heat supply systems for a multi-effect seawater distillation unit. In ISES Solar World Congress, Göteborg, Sweden.